36th AIAA Thermophysics Conference
23-26 June 2003, Orlando, Florida

AIAA 2003-3783

AIAA 2003–3783

Assessment of Entropy Generation Rate as a Predictor of Continuum Breakdown

Po-Heng Chen and Iain D. Boyd
Department of Aerospace Engineering
University of Michigan, Ann Arbor, MI 48109

José A. Camberos
U.S. Air Force Research Laboratory
Wright–Patterson Air Force Base, Dayton, OH 45433

36th AIAA Thermophysics Conference
June 23–26, 2003/Orlando, FL

Assessment of Entropy Generation Rate as a Predictor of Continuum Breakdown

Po-Heng Chen* and Iain D. Boyd†
Department of Aerospace Engineering
University of Michigan, Ann Arbor, MI 48109

José A. Camberos‡
U.S. Air Force Research Laboratory
Wright–Patterson Air Force Base, Dayton, OH 45433

Hybrid methods employing a combination of continuum and particle methods are being developed for a variety of applications from hypersonic to micro-scale flows. A key issue in the development of such hybrid methods is the determination of when to use the continuum and particle flow descriptions. This is most commonly performed by consideration of a continuum breakdown parameter that indicates failure of the continuum approach. In the present study, the entropy generation rate is evaluated as a continuum breakdown parameter for several different flows including a flat plate boundary layer, normal shock waves, and a complex hypersonic flow. The basic motivation for the study is the observation that entropy production provides a strong physical basis for detection of non-continuum phenomena. Comparisons are made between breakdown parameters based on the entropy generation rate and other parameters based on flow field gradients. The results indicate that breakdown parameters based on entropy generation exhibit many of the same features as the existing parameters.

Nomenclature

c	Sound speed, m/s
c_p	Specific heat at constant pressure
Kn	Knudsen number-like breakdown parameter
ℓ	Reference length, m
L	Reference length on cylinder/flare, m
M	Mach number
p	Pressure, Pa
q_j	Heat flux vector, W/m^2
Re_s	Reynolds number based on length s
$\dot{S}_{gen}$	Entropy generation rate, $\frac{J}{K \cdot m^3 \cdot s}$
T	Temperature, K
u	Velocity, m/s
U	Reference velocity, m/s
x, y, z	Cartesian body axes, m
η	Wall-normal distance, non-dimensionalized
κ	Coefficient of thermal conductivity
μ	Coefficient of viscosity
Θ	Temperature, non-dimensionalized
ρ	Density, kg/m^3
ψ	Streamfunction
$\tau_{i,j}$	Stress tensor, N/m^2

Subscripts

0	Reference
1	Upstream
2	Downstream
S	based on $\dot{S}_{gen}$
w	Wall
∞	Freestream

*Graduate Student Research Assistance, AIAA Student Member (chenph@umich.edu)

†Professor, AIAA Associate Fellow (iainboyd@umich.edu)

‡Aerospace Engineer, AIAA Senior Member.

Introduction

THE development of hypersonic vehicles is of particular interest to both military[1] and commercial[2] aviation. Unfortunately, hypersonic experimentation in a laboratory or wind tunnel is difficult and flight tests are expensive. Therefore computational methods, such as Computational Fluid Dynamics (CFD) and the Direct Simulation Monte Carlo method (DSMC), will serve as critical tools in the design of hypersonic vehicles.[3]

While CFD works well in subsonic, sonic, and supersonic regimes, it introduces significant errors under rarefied conditions in the hypersonic regime due to the breakdown of continuum properties, i.e. the assumption of a fluid continuum becomes invalid in a rarefied gas.[4] DSMC has proven to be an excellent method for predicting flows of rarefied gas but is significantly more expensive than CFD computationally.[5] One solution is to introduce a hybrid code that combines both CFD and DSMC. There are two challenges in combining CFD and DSMC. The first is determining when to use one method or the other. The second is sharing computational data between the two methods at their boundaries.[6] The present study focuses on the first

problem by exploring a continuum breakdown parameter. For the continuum breakdown parameter, several candidates based on the Knudsen number have been reviewed by Wang and Boyd.[5] This study proposes the use of *entropy generation rate* as a continuum breakdown parameter since it has a stronger physical foundation than Knudsen numbers.

The entropy generation rate is defined as follows:[7]

$$\dot{S}_{gen} = \frac{\tau_{ji}}{T}\frac{\partial u_i}{\partial x_j} - \frac{q_j}{T^2}\frac{\partial T}{\partial x_j} \tag{1}$$

This concept can be applied to continuum thermodynamics through the Navier-Stokes equations.[8] These equations for the conservation of mass, momentum, and energy, respectively, are:

$$\frac{\partial \rho}{\partial t} + \nabla \cdot \rho V = 0 \tag{2}$$

$$\rho \frac{D\mathbf{V}}{Dt} = \rho \mathbf{g} + \nabla \cdot \tau_{ij} - \nabla p \tag{3}$$

$$\rho \frac{Dh}{Dt} = \frac{Dp}{Dt} + \nabla \cdot (\kappa \nabla T) + \tau_{ij}\frac{\partial u_i}{\partial x_j} \tag{4}$$

Three configurations are chosen for this study: a laminar boundary layer flow over a flat plate, normal shock waves, and a hypersonic flow over a hollow cylinder/flare configuration. The first case focuses on the extreme gradients that would be present on the surface of any vehicle. The second case focuses on the extreme gradients present across the shock waves of any supersonic vehicle. The third case focuses on a configuration that resembles the flight conditions on a hypersonic vehicle.

Laminar Boundary Layer over a Flat Plate

Laminar boundary layer flow over a flat plate is a classic problem for which there is an established solution by Blasius.

Analytical Solution

The solution for the laminar boundary layer over a flat plate makes the following assumptions:

1. The flow is incompressible, viscous, and two-dimensional.
2. No-slip condition at the surface ($u = v = 0$ at $y = 0$) and freestream conditions far from the plate ($u = u_\infty$ at $y = \infty$).
3. Buoyancy effects are negligible so temperature and velocity are not coupled.

We start with the steady and incompressible continuity and momentum equations, respectively, in two space dimensions:

$$\frac{\partial u}{\partial x} + \frac{\partial v}{\partial y} = 0 \tag{5}$$

$$u\frac{\partial u}{\partial x} + v\frac{\partial u}{\partial y} = U\frac{dU}{dx} + \nu\frac{\partial^2 u}{\partial y^2} \tag{6}$$

with the boundary conditions $u(x,0) = v(x,0) = 0$ and $u(x,\infty) = U(x)$.

Substituting the dimensionless similarity variables

$$\eta = y\sqrt{\frac{U}{2\nu x}} \tag{7}$$

$$\psi = \sqrt{2\nu U x} f(\eta) \tag{8}$$

into the momentum equation (6), we can manipulate the equation until it yields the following differential equation:[9]

$$f''' + ff'' = 0 \tag{9}$$

with boundary conditions $f(0) = 0$, $f'(0) = 0$, $f'(\infty) = 1$. Using a Runge-Kutta solver, the velocity profile solution is obtained.

A similar technique is used to solve for the energy equation:

$$\rho c_p \left(u\frac{\partial T}{\partial x} + v\frac{\partial T}{\partial y}\right) \approx \kappa\frac{\partial^2 T}{\partial y^2} + \mu\left(\frac{\partial u}{\partial y}\right)^2 \tag{10}$$

where the dimensionless similarity variable for temperature is:

$$\Theta(\eta) = \frac{T - T_\infty}{T_w - T_\infty} \tag{11}$$

Although White[9] assumed a negligible Eckert number Ec, we derive the more general solution:

$$\Theta'' + \Pr f\Theta' + \Pr \mathrm{Ec} f''^2 = 0 \tag{12}$$

A Runge-Kutta solver is used again to obtain the solution. For this solution, the non-dimensionalized entropy generation rate can be expressed as:

$$\begin{aligned}\dot{S}^*_{gen}\frac{x}{\rho U c_p} = {} & \tfrac{1}{2}\mathrm{Ec} f''^2\left(\tfrac{T_w}{T_\infty} - 1\right)\left(1 + \tfrac{\Delta T}{T_\infty}\Theta\right)^{-1} \\ & + \tfrac{1}{2}\Pr{}^{-1}\Theta'^2\left(\tfrac{T_w}{T_\infty} - 1\right)^2\left(1 + \tfrac{\Delta T}{T_\infty}\Theta\right)^{-2}\end{aligned} \tag{13}$$

where $\Delta T = T_w - T_\infty$ and Eckert number $\mathrm{Ec} = \frac{U^2}{c_p \Delta T}$.

CFD Solution

The CFD package used is *Cobalt*$_{60}$.[10] It was developed by the United States Air Force at the Air Force Research Laboratory at Wright-Patterson Air Force Base in Dayton, Ohio. The flat plate case is run using the laminar Navier-Stokes equations under the following conditions: $Re_L = 10^5$, $p = 2{,}174\ N/m^2$,

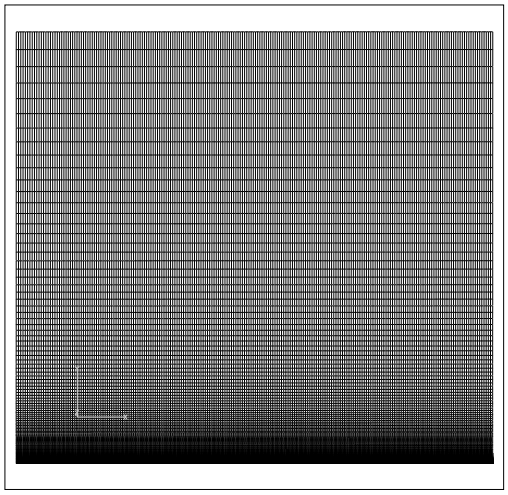

Fig. 1 Mesh for flat plate.

$T = 288.15\ K$, and $M = 0.20$. The grid is shown in Fig. 1 and reveals the general packing of the mesh toward the flat plate at the bottom. The bottom surface starts from the left with a slip plane of length 0.1 m with 20 points followed by the flat plate of unit length with 200 points. From top to bottom, there are 100 points.

The velocity profiles in Fig. 2 show that the Blasius and *Cobalt*$_{60}$ solutions match very well. Similarly, the temperature and entropy generation rate profiles plotted in Figs. 3 and 4 indicate good agreement between computation and theory. Here, the entropy generation rate is non-dimensionalized using the following form suggested by Camberos and Chen:[14]

$$Kn_S \equiv \frac{\ell \dot{S}_{gen}}{\rho R \sqrt{RT}} \tag{14}$$

where ℓ is taken to be the local mean free path λ. The data from the flat plate case indicate that the entropy generation rate formulae as implemented in *Cobalt*$_{60}$ accurately match the analytical solutions.

Normal Shock Waves

The normal shock wave is a classic flow problem involving non-isentropic gas dynamics with well established solutions. The Rankine-Hugoniot jump equations give upstream and downstream values. Integration over the basic one-dimensional Navier-Stokes equations yield profiles, as shown by Gilbarg and Paolucci.[11]

Analytical and Numerical Solutions for Air

The solution for the shock wave profiles assumes that the flow is compressible and one-dimensional. Runge-Kutta integration is used over the following one-dimensional Navier-Stokes equations:

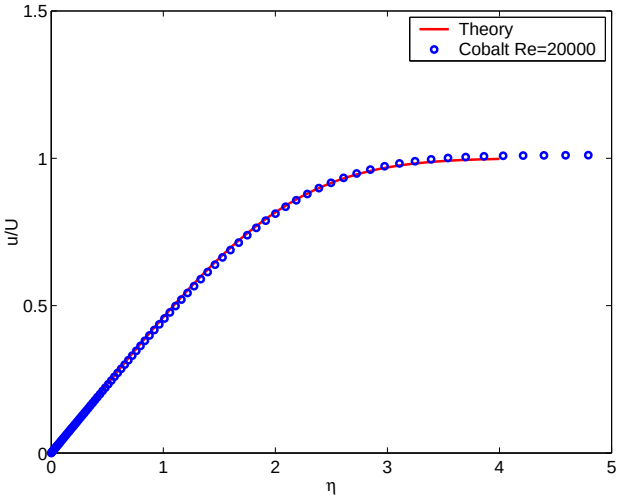

Fig. 2 Velocity profiles of Blasius and *Cobalt*$_{60}$ solutions.

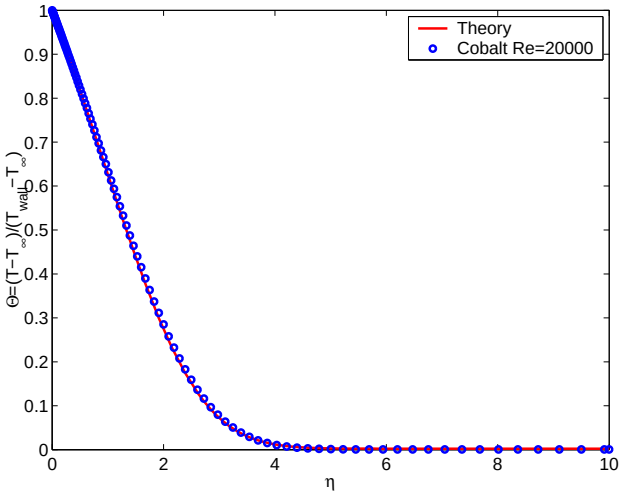

Fig. 3 Temperature profiles of analytical and *Cobalt*$_{60}$ solutions.

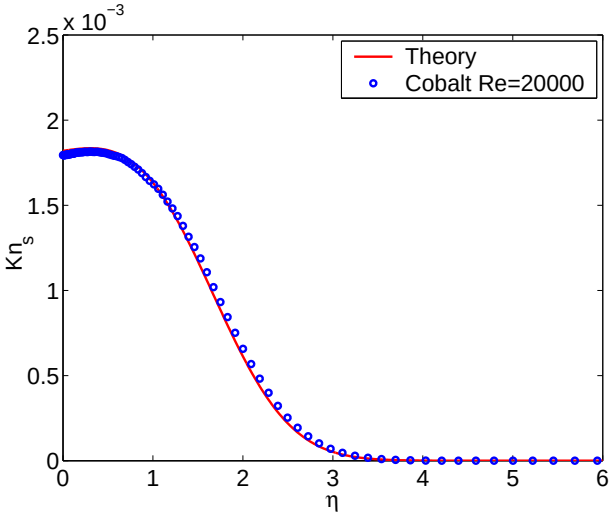

Fig. 4 Entropy generation rate profiles of analytical and *Cobalt*$_{60}$ solutions.

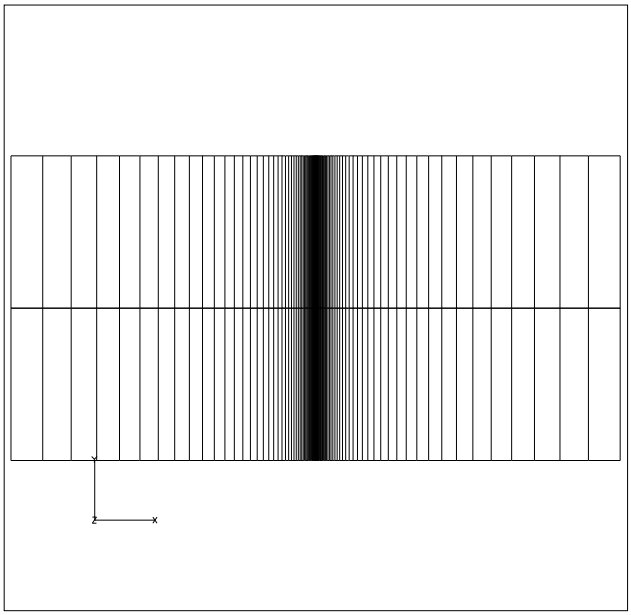

Fig. 5 Mesh for a normal shock wave.

$$C_1\left(1-\frac{RT}{u^2}\right)\frac{du}{dx}+C_1\frac{R}{u}\frac{dT}{dx}-\frac{d\tau}{dx}=0 \qquad (15)$$

$$C_1\left(u-\frac{\tau}{c_1}\right)\frac{du}{dx}+C_1c_p\frac{dT}{dx}-u\frac{d\tau}{dx}+\frac{dq}{dx}=0 \qquad (16)$$

$$\frac{4}{3}\mu\frac{du}{dx}-\tau=0 \qquad (17)$$

$$\kappa\frac{dT}{dx}+q=0 \qquad (18)$$

where the invariant $C_1=\rho u$.

It can be shown that in the temperature-velocity solution space, the supersonic upstream condition is a nodal point while the subsonic downstream condition is a saddle point.[11,12] Therefore integration from the upstream condition to the downstream condition, as intuition would have us do, is unstable and would yield inaccurate results. However, by integrating in the reverse direction, a stable solution results. For this case, a version of $Cobalt_{60}$ is customized to initialize each half of the flow with values from given parameters and the jump equations so that any shock waves form and stay in the center of the flow.

The mesh for the flow is shown in Fig. 5 with points clustered at the shock interface. There are 100 points lengthwise and only 3 points in the normal direction. In the results that follow, the gas is air and the upstream conditions are: $M_1=2.0$, $p_1=1,172\ N/m^2$, and $T_1=226.6\ K$. The velocity and temperature profiles shown in Fig. 6 and 7, respectively, indicate good agreement between the two solutions.

The entropy generation rate is shown in Fig. 8. These results indicate good agreement between the analytical results and the computation. They also show

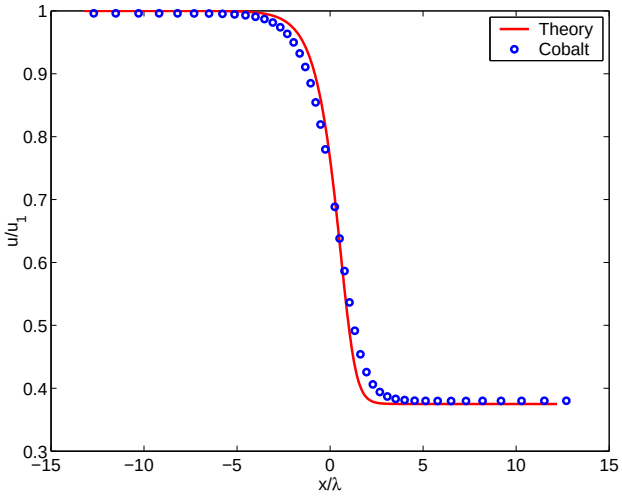

Fig. 6 Velocity profile in a normal shock wave.

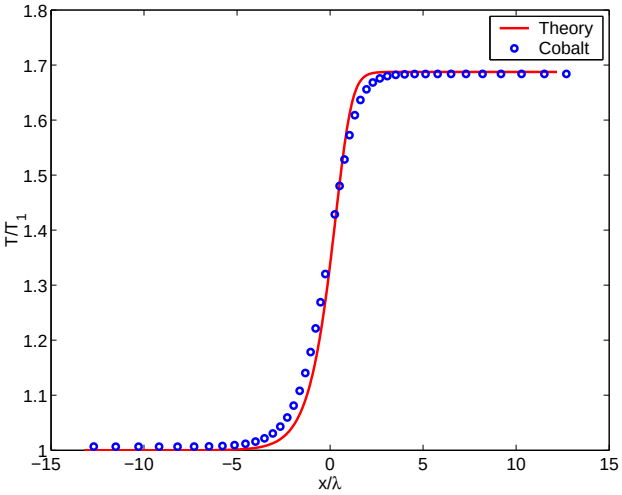

Fig. 7 Temperature profile in a normal shock wave.

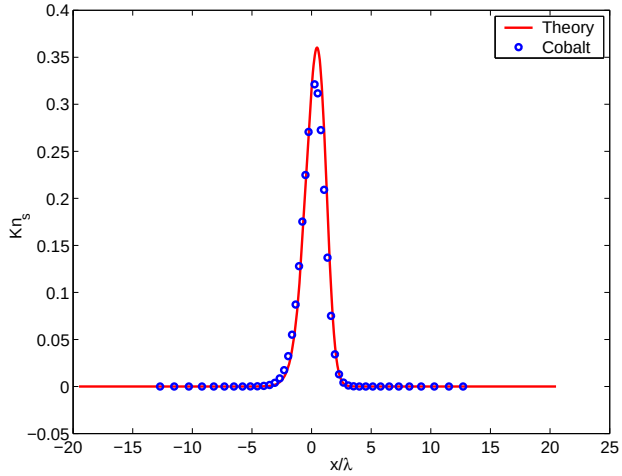

Fig. 8 Entropy generation rate profile in a normal shock wave.

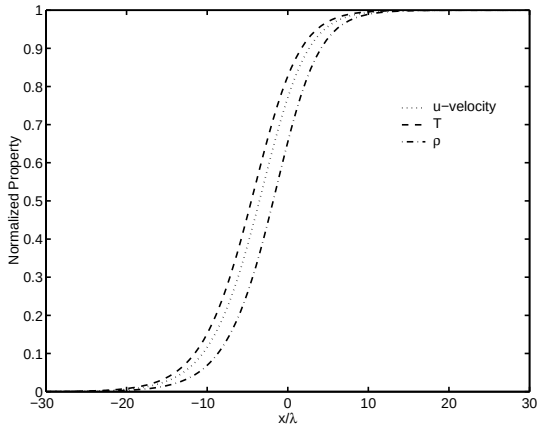

Fig. 9 Normalized flow properties across a normal shock wave at $M = 1.55$ in Argon.

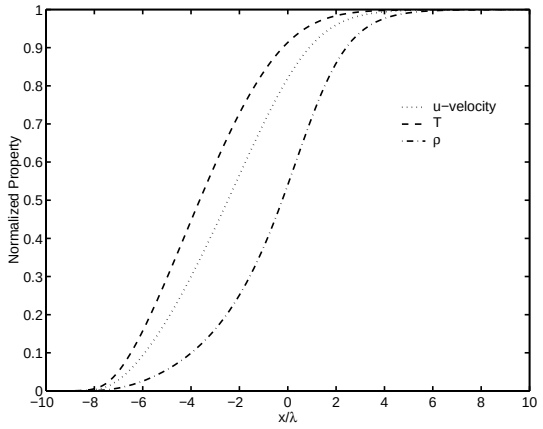

Fig. 10 Normalized flow properties across a normal shock wave at $M = 10$ in Argon.

that the entropy generation rate reaches a sharp peak in the middle of the shock wave front. This is a region of strong nonequilibrium where continuum methods may fail.

Analysis of Argon Flows

To assess the entropy generation rate as a continuum breakdown parameter, we consider the solutions of the Navier–Stokes equations taken from Boyd et al.[13] for normal shock waves at Mach 1.55 and Mach 10 in Argon. Figures 9 and 10 show normalized values of velocity, temperature, and density for Mach 1.55 and Mach 10, respectively.

The research of Wang and Boyd[5] found that the following represented an effective continuum breakdown parameter for hypersonic flows:

$$Kn_{\max} \equiv \max(Kn_D, Kn_T, Kn_V) \qquad (19)$$

with a threshold of 0.05, where for $Q = D, T, V$:

$$Kn_Q = \frac{\lambda}{Q} |\nabla Q| \qquad (20)$$

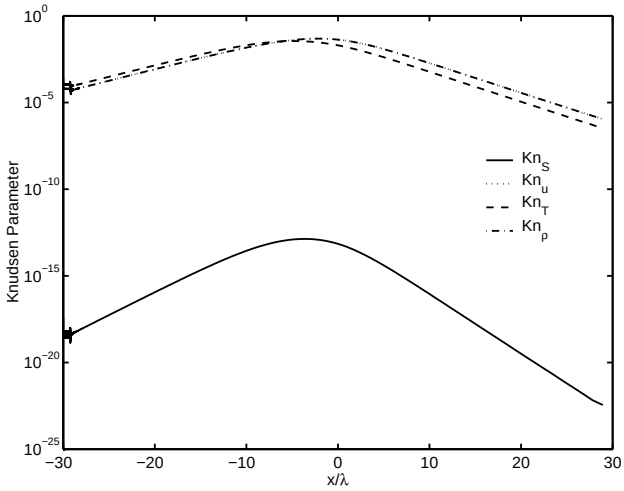

Fig. 11 Breakdown parameters across a normal shock wave at $M = 1.55$ in Argon.

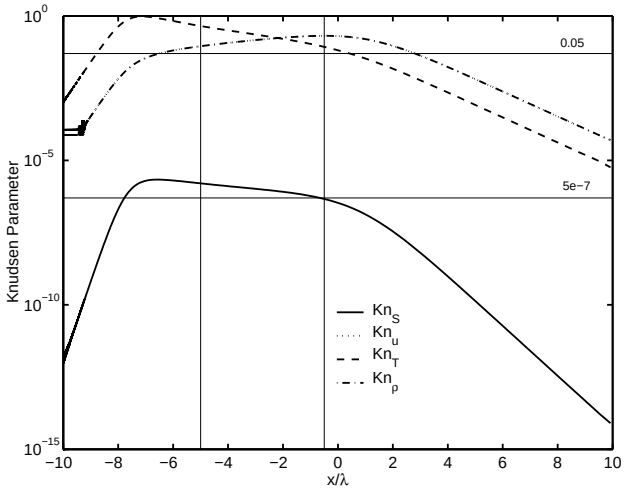

Fig. 12 Breakdown parameters across a normal shock wave at $M = 10$ in Argon with continuum breakdown assumed between the two vertical lines.

Here the D, T, and V stand for density, temperature, and velocity, respectively.

The entropy generation rate parameter, Eq. (14), and the Knudsen number parameters, Eq. (20), are shown in Figs. 11 and 12 for Mach 1.55 and Mach 10, respectively. In both cases, the entropy generation rate parameter resembles the shape of the temperature-based Knudsen parameter, although significantly lower in magnitude.

The results of Boyd et al.[13] show a difference greater than 5 percent between the Navier-Stokes and DSMC results for density and temperature in the Mach 10 shock wave. This 5 percent error is assumed to indicate continuum breakdown. The region where density difference between Navier-Stokes and DSMC is greater than 5 percent is indicated in Fig. 12 as the region between the two vertical lines. The upper horizontal line in the same plot indicates the breakdown threshold of 0.05 used by Boyd et al. for their parameters. It

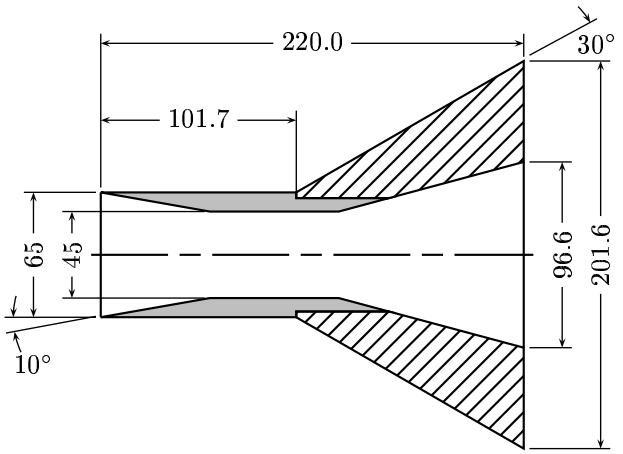

Fig. 13 Hollow cylinder/flare geometry.

slightly over-predicts the shock thickness for density. The lower horizontal line is the entropy generation rate parameter threshold of 5×10^{-7} and it over-predicts the width of the breakdown region as well. From these results, the entropy generation rate Knudsen parameter seems to predict the breakdown region in a similar way to the density-based Knudsen parameter.

Hypersonic Flow Over a Hollow Cylinder/Flare Geometry

The hollow cylinder/flare geometry shown in Fig. 13 represents a typical configuration that may be found on a section of a hypersonic vehicle. The CFD data that is analyzed here consists of a solution of the Navier–Stokes equations and is taken from Wang and Boyd[5] for flow conditions of: ρ_∞=5.07×10^{-4} kg/m^3, U_∞=2,609 m/s, T_∞=129 K giving M_∞=11.3. The reference length L corresponds to the cylinder section of length 101.7 *mm* in the figure.

A contour plot of the entropy generation rate, Eq. (1), is shown in Fig. 14. Note the shock wave from the lip of the cylinder followed by its reflection off the flared wall and the "bubble" at the intersection of the walls.

In the following analysis, the continuum breakdown regions are assumed to be those where any difference (error) greater than 5 percent between the Navier-Stokes and DSMC results are noted for any density, velocity, or temperature. The DSMC solution is also from Wang and Boyd.[5]

The data from near the tip of the cylinder (x/L = 0.01) is shown in Fig. 15 with continuum breakdown assumed left of the vertical line. By inspection, the Knudsen parameter based on entropy generation rate, Eq. (14), does not seem to be useful in predicting breakdown in this case. However, two more non-dimensionalizations of entropy generation rate are plotted in Fig. 16. The form of the non-dimensionalization is:

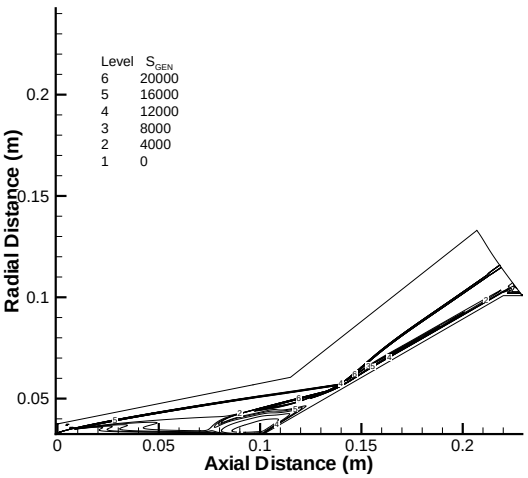

Fig. 14 Entropy generation rate contours.

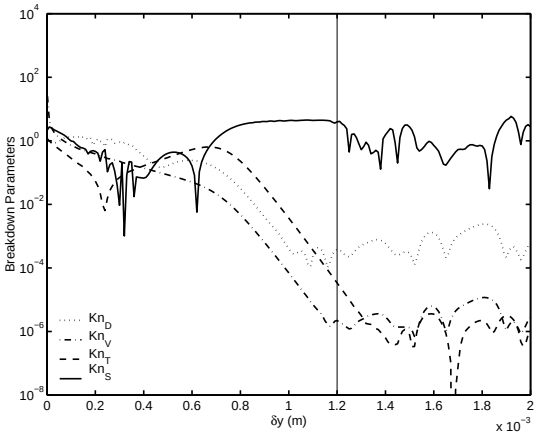

Fig. 15 Breakdown parameters based on basic properties at x/L = 0.01. Breakdown indicated in the region to the left of the vertical line.

$$S_{GEN_{normLocal}} = \frac{\dot{S}_{gen}}{\rho u R/\lambda} \tag{21}$$

$$S_{GEN_{normGlobal}} = \frac{\dot{S}_{gen}}{\rho_0 U R/\ell} \tag{22}$$

where the former uses local and the latter uses global freestream values. The local reference length is taken to be the mean free path whereas the global reference length is the length of the cylinder L. These two non-dimensionalizations seem to resemble Kn_{MAX} in shape. The proposed threshold levels for these two parameters are plotted in Fig. 17. The global parameter threshold is proposed to be 1 while the local parameter threshold is proposed to be 5×10^{-4}. In this case, all three parameters predict a region of continuum breakdown that is wider than the comparison of DSMC and CFD solutions actually indicates.

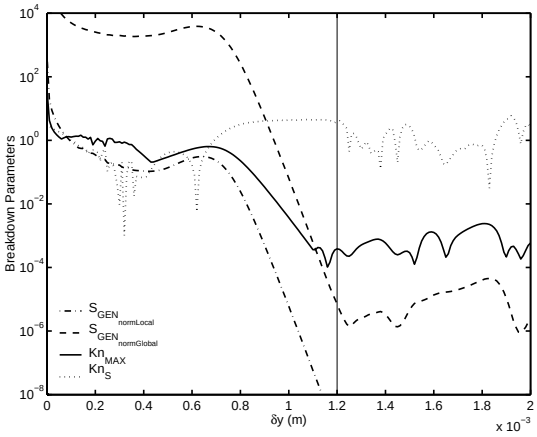

Fig. 16 Comparison of breakdown parameters at $x/L = 0.01$. Breakdown indicated in the region to the left of the line.

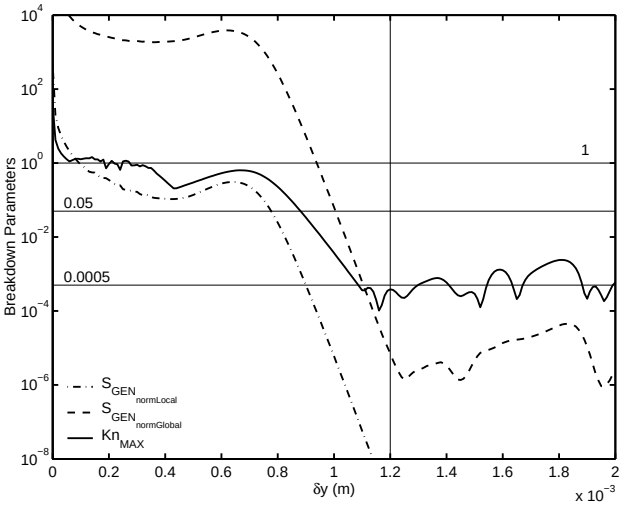

Fig. 17 Comparison of breakdown parameters at $x/L = 0.01$ with thresholds. Breakdown indicated in the region to the left of the line.

The data from the middle of the cylinder ($x/L = 0.50$) is shown in Fig. 18 with continuum breakdown assumed in the two leftmost regions. The error in the first region is relatively insignificant, but still above 5 percent. The error spikes in the second region. By inspection in Fig. 19, the Knudsen parameter based on entropy generation rate does not seem to be useful in predicting breakdown in this case either. The proposed thresholds in Fig. 20 show relatively good agreement to breakdown region boundaries. All three parameters predict the continuum breakdown observed in the shock front and then indicate a region of continuum flow on the other side of the shock that is not found in the flow solutions. A large region of non-continuum flow is then predicted by all three parameters towards the cylinder surface.

The data at the intersection between the cylinder and the flare ($x/L = 1.00$) is shown in Fig. 21

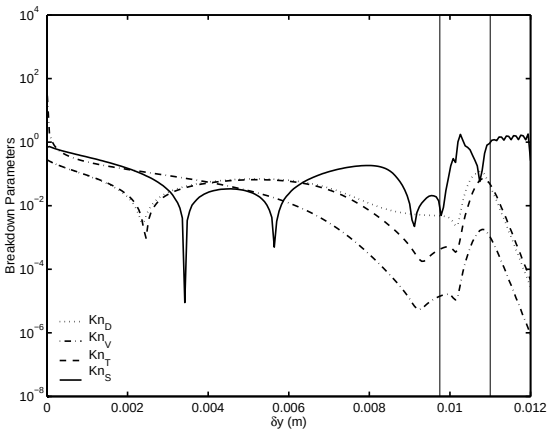

Fig. 18 Breakdown parameters based on basic properties at $x/L = 0.50$. Breakdown indicated in the leftmost two regions.

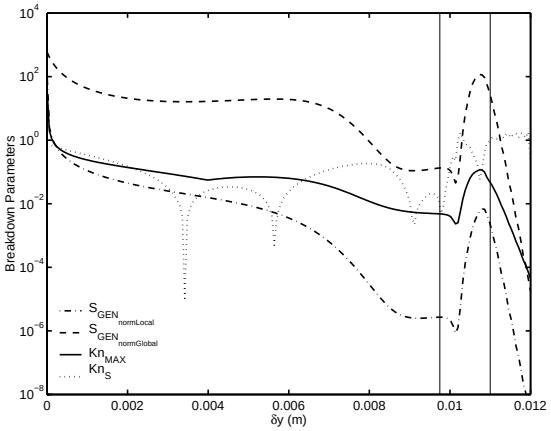

Fig. 19 Comparison of breakdown parameters at $x/L = 0.50$. Breakdown indicated in the leftmost two regions.

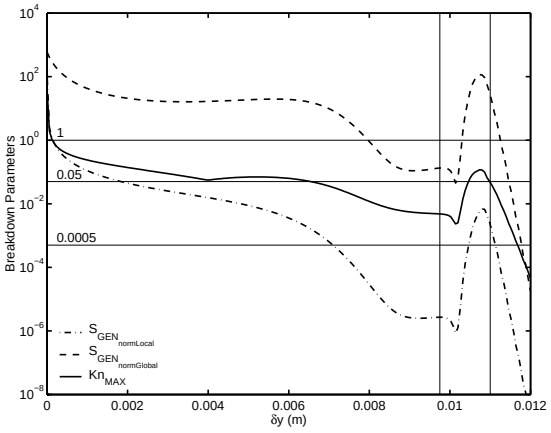

Fig. 20 Comparison of breakdown parameters at $x/L = 0.50$ with thresholds. Breakdown indicated in the leftmost two regions.

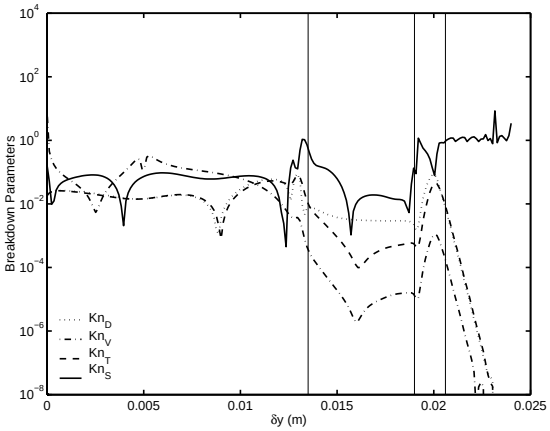

Fig. 21 Breakdown parameters based on basic properties at $x/L = 1.00$. Breakdown indicated in the first and third regions from the left.

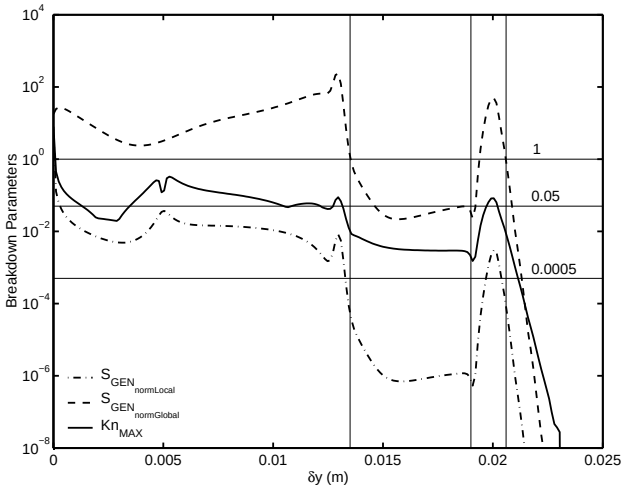

Fig. 23 Comparison of breakdown parameters at $x/L = 1.00$ with thresholds. Breakdown indicated in the first and third regions from the left.

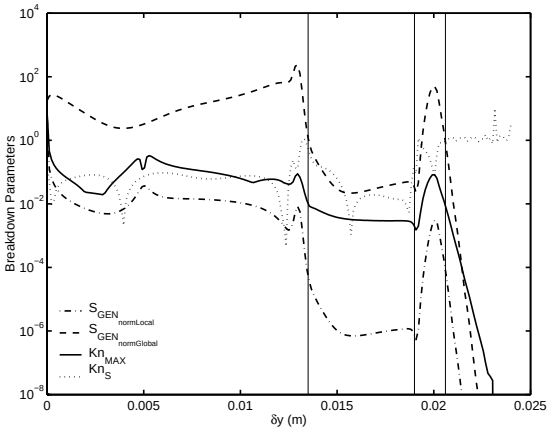

Fig. 22 Comparison of breakdown parameters at $x/L = 1.00$. Breakdown indicated in the first and third regions from the left.

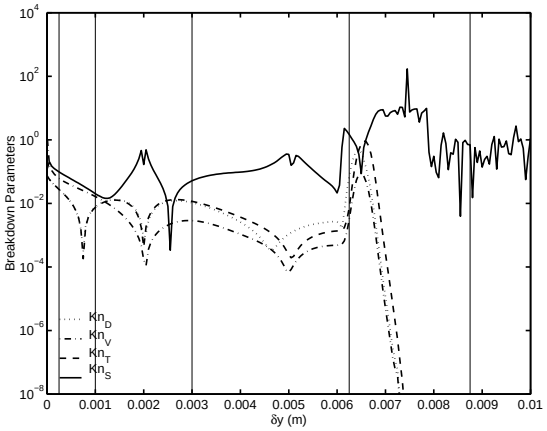

Fig. 24 Breakdown parameters based on basic properties at $x/L = 1.60$. Breakdown indicated in the first, third, and fifth regions from the left.

with continuum breakdown assumed in the first and third regions from the left. By inspection in Fig. 22, the Knudsen parameter based on entropy generation rate does not seem promising for predicting breakdown in this case either. The proposed thresholds in Fig. 23 show very good agreement to breakdown region boundaries both around the shock front and as the surface is approached.

The data from midway along the flare ($x/L = 1.60$) is shown in Fig. 24 with continuum breakdown assumed in the first, third,and fifth regions from the left. Once again, the Knudsen parameter based on entropy generation rate in Fig. 25 is not useful here. Disappointingly, the proposed thresholds for the breakdown parameters shown in Fig. 26 do not work well. They predict continuum breakdown around the shock front in a region that is considerably smaller than the DSMC and CFD solutions suggest. The parameters also fail to predict continuum breakdown in the third region. It is important to note that these problems are also encountered by the Knudsen number parameter of Wang and Boyd.[5]

It is interesting to note that in Fig. 25, the earlier entropy generation rate Knudsen parameter shows an upturn where the third region is. Although no threshold line can be drawn to take advantage of this parameter, perhaps a different threshold criteria can be established to make this parameter useful.

Concluding Remarks

The entropy generation rate has been proposed as a candidate parameter to detect breakdown of the continuum assumption in computations of nonequilibrium gas flows. In the present study, a number of different parameters based on the entropy generation rate were proposed. The usefulness of these parameters in predicting continuum breakdown was assessed using a number of different configurations representative

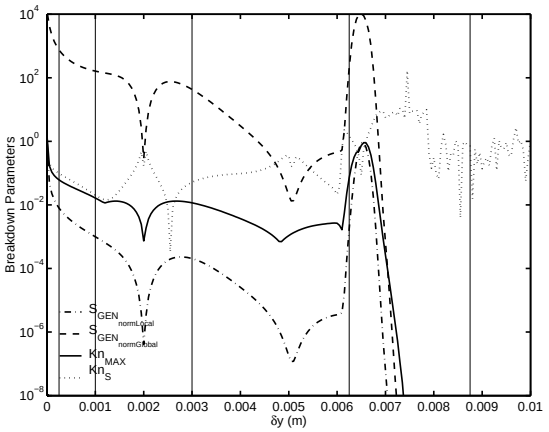

Fig. 25 Comparison of breakdown parameters at $x/L = 1.60$. Breakdown indicated in the first, third, and fifth regions from the left.

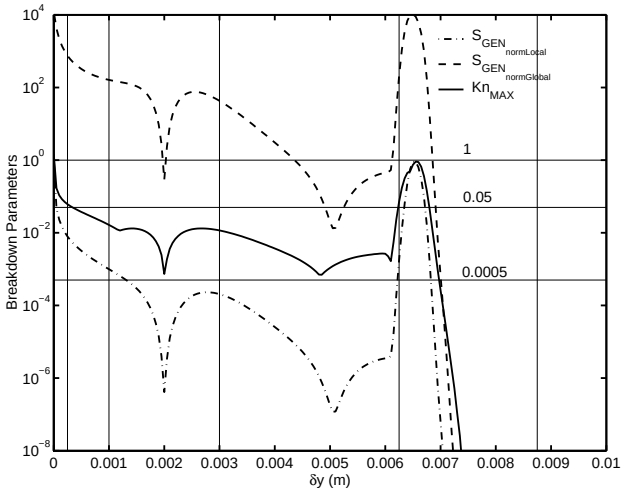

Fig. 26 Comparison of breakdown parameters at $x/L = 1.60$ with thresholds. Breakdown indicated in the first, third, and fifth regions from the left.

of flows about a hypersonic vehicle. Two relatively simple flows were first considered: a boundary layer flow and one dimensional shock waves. In addition, a complex hypersonic flow about a cylinder–flare configuration was investigated.

These studies showed that the entropy generation rate can indicate non-continuum phenomena associated with sharp gradients and therefore demonstrated some promise as a continuum breakdown parameter. Comparisons between the Knudsen-based parameter and the entropy generation rate parameter were made from several CFD data sets including new solutions obtained with *Cobalt*$_{60}$ and with solutions of the Navier–Stokes equations published earlier in Boyd et al.[13] and Wang and Boyd.[5] The results showed that parameters based on entropy generation rate are about as useful as those based on density, velocity, and temperature gradients. It may be argued that a breakdown parameter based on entropy production has a more solid theoretical basis than those parameters based on general flow field gradients. However, all of the breakdown parameters considered failed to predict non-continuum behavior in the shock front indicating the need for further investigation.

Acknowledgments

This work was sponsored by the Air Force Office of Scientific Research (AFOSR) through grant F49620–01–1–0003 to the University of Michigan monitored by Dr. John Schmisseur, and through grant 2307N32A to the Air Force Research Laboratory at Wright-Patterson Air Force Base. The views and conclusions contained herein are those of the authors and should not be interpreted as necessarily representing the official policies or endorsements, either expressed or implied, of the AFOSR or the U.S. Government.

References

[1] "Review and Evaluation of the Air Force Hypersonic Technology Program," Tech. rep., U.S. Air Force, 2101 Constitution Ave, N.W.; Washington, D.C. 20418, 1998.

[2] "Aeronautical Technologies for the Twenty-First Century," Tech. rep., National Air and Space Administration, 2101 Constitution Ave, N.W.; Washington, D.C. 20418, 1992.

[3] "Hypersonic Technology for Military Application," Tech. rep., U.S. Air Force, 2101 Constitution Ave, N.W.; Washington, D.C. 20418, 1989.

[4] Bird, G. A., *Molecular Gas Dynamics and the Direct Simulation of Gas Flows*, No. 42 in Oxford Engineering Science Series, Oxford University Press, 1994.

[5] Wang, W.-L. and Boyd, I. D., "Predicting Continuum Breakdown in Hypersonic Viscous Flows," *Physics of Fluids*, Vol. 15, 2003, pp. 91–100.

[6] Wang, W.-L., Sun, Q., and Boyd, I. D., "Towards Development of a Hybrid DSMC–CFD Method for Simulating Hypersonic Interacting Flows," AIAA Paper 2002–3099, June 2002, St. Louis, MO.

[7] Camberos, J. A., "On the Construction of Entropy Balance Equations for Arbitrary Thermophysical Processes," AIAA Paper 2001–0815, Jan. 2001, Reno, NV.

[8] Camberos, J. A., "On the Construction of Exergy Balance Equations for Availability Analyses," AIAA Paper 2002–2880, June 2002, St. Louis, MO.

[9] White, F. M., *Viscous Fluid Flow*, McGraw–Hill Series in Mechanical Engineering, McGraw–Hill, 2nd ed., 1991.

[10] Grismer, M. J., Strang, W. Z., Tomaro, R. F., and Witzeman, F. C., "Cobalt: A parallel, implicit, unstructured Euler/Navier–Stokes Solver," *Advances in Engineering Software*, Vol. 29, No. 3–6, 1998, pp. 365–373.

[11] Gilbarg, D. and Paolucci, D. A., "The Structure of Shock Waves in the Continuum Theory of Fluids," *Journal of Rational Mechanics and Analysis*, Vol. 2, No. 4, 1953, pp. 617–642.

[12] Canupp, P. W., "The Influence of Magnetic Fields for Shock Waves and Hypersonic Flows," AIAA Paper 2000–2260, 2000.

[13] Boyd, I. D., Chen, G., and Candler, G. V., "Predicting Failure of the Continuum Fluid Equations in Transitional Hypersonic Flows," *Physics of Fluids*, Vol. 7, 1995, pp. 210–219.

[14] Camberos, J. A. and Chen, P.-H., "Continuum Breakdown Parameter Based on Entropy Generation Rates," AIAA Paper 2003–0157, Jan. 2003, Reno, NV.